

One-Step Photoactivation of a Dual-Functionalized Bioink as Cell Carrier and Cartilage-Binding Glue for Chondral Regeneration

Khoon S. Lim, Florencia Abinzano, Paulina Nuñez Bernal, Ane Albillos Sanchez, Pau Atienza-Roca, Iris A. Otto, Quentin C. Peiffer, Michiya Matsusaki, Tim B. F. Woodfield, Jos Malda, and Riccardo Levato**

Cartilage defects can result in pain, disability, and osteoarthritis. Hydrogels providing a chondroregeneration-permissive environment are often mechanically weak and display poor lateral integration into the surrounding cartilage. This study develops a visible-light responsive gelatin ink with enhanced interactions with the native tissue, and potential for intraoperative bioprinting. A dual-functionalized tyramine and methacryloyl gelatin (GelMA-Tyr) is synthesized. Photo-crosslinking of both groups is triggered in a single photoexposure by cell-compatible visible light in presence of tris(2,2'-bipyridyl)dichlororuthenium(II) and sodium persulfate as initiators. Neo-cartilage formation from embedded chondroprogenitor cells is demonstrated in vitro, and the hydrogel is successfully applied as bioink for extrusion-printing. Visible light in situ crosslinking in cartilage defects results in no damage to the surrounding tissue, in contrast to the native chondrocyte death caused by UV light (365–400 nm range), commonly used in biofabrication. Tyramine-binding to proteins in native cartilage leads to a 15-fold increment in the adhesive strength of the biogel compared to pristine GelMA. Enhanced adhesion is observed also when the ink is extruded as printable filaments into the defect. Visible-light reactive GelMA-Tyr bioinks can act as orthobiologic carriers for in situ cartilage repair, providing a permissive environment for chondrogenesis, and establishing safe lateral integration into chondral defects.


1. Introduction

Articular cartilage defects are a major problem in the orthopedic field, affecting 36% of athletes and 16% of patients that underwent arthroscopic investigation following pain complaints.^[1] These cartilage injuries can cause disability in patients, greatly affecting their quality of life and exerting significant impact on overall healthcare costs. When left untreated, cartilage defects can lead to early-onset osteoarthritis and higher risk of knee replacement surgery.^[2] Current treatment options are limited and often result in the formation of fibrotic tissue that exhibits lesser quality than native articular cartilage and increased propensity toward degeneration.^[3]

In recent years, injectable hydrogels have risen as promising candidates for cartilage repair. This is due to their highly hydrated microenvironment, which mimics the native extracellular matrix (ECM) and allows effective transfer of various solutes and nutrients.^[4] Furthermore, these hydrogels normally provide a biocompatible and/or biodegradable structure that enables

Dr. K. S. Lim, P. Atienza-Roca, Prof. T. B. F. Woodfield
Christchurch Regenerative Medicine and Tissue Engineering (CReaTE)
Group and Medical Technologies Centre of Research Excellence
(MedTech CoRE)
Department of Orthopaedic Surgery and Musculoskeletal Medicine
University of Otago Christchurch
2 Riccarton Ave, Christchurch 8140, New Zealand
E-mail: khoon.lim@otago.ac.nz

F. Abinzano, P. N. Bernal, A. Albillos Sanchez, I. A. Otto, Q. C. Peiffer,
Prof. J. Malda, Dr. R. Levato
Department of Orthopaedics and Regenerative Medicine Center
University Medical Center Utrecht
Utrecht University
Heidelberglaan 100, Utrecht 3584 CX, The Netherlands
E-mail: r.levato-2@umcutrecht.nl
Prof. M. Matsusaki
Department of Applied Chemistry
Graduate School of Engineering
Osaka University
2-1 Yamadaoka, Suita, Osaka 565-0871, Japan
Prof. J. Malda, Dr. R. Levato
Department of Clinical Sciences
Faculty of Veterinary Medicine
Utrecht University
Yalelaan 1, Utrecht 3584 CL, The Netherlands

 The ORCID identification number(s) for the author(s) of this article can be found under <https://doi.org/10.1002/adhm.201901792>

© 2020 The Authors. Published by WILEY-VCH Verlag GmbH & Co. KGaA, Weinheim. This is an open access article under the terms of the Creative Commons Attribution-NonCommercial License, which permits use, distribution and reproduction in any medium, provided the original work is properly cited and is not used for commercial purposes.

DOI: 10.1002/adhm.201901792

cell encapsulation and delivery of bioactive molecules to targeted sites for cartilage regeneration.^[5] Bioactive hydrogel formulations show promise as clinically translatable new therapies, with two formulations currently undergoing clinical trials to obtain FDA approval: GelrinC (Regentis Biomaterials), a cell-free hydrogel composed of poly(ethylene glycol)-diacrylate (PEG-DA) and denatured fibrinogen, designed to be photo-crosslinked in situ at the site of the defect; and CARTISTEM (Medipost), which is an injectable product composed an allogeneic human umbilical cord blood-derived mesenchymal stem cells mixed in a hyaluronic acid hydrogel and approved for clinical use in South Korea since 2012.^[6]

An ideal hydrogel for cartilage regeneration should be able to mimic 3D environment of cartilage ECM, support the development of neo-cartilage matrix, and integrate with the surrounding native tissue. Moreover, articular cartilage in joints has a specific zonal orientation (superficial, middle, deep, and calcified zones), in which cell morphology, biomarker expression profiles, matrix composition, and mechanical properties vary in a depth-dependent fashion.^[7,8] Biofabrication technologies, which enable precise control over the spatial deposition of cells and bioactive cues by means of bioprinting and bioassembly, have emerged as promising strategies to recapitulate such in vivo native architectures,^[9–14] for instance by the controlled extrusion of hydrogel-based bioinks via layer-by-layer deposition.^[16] Importantly, via controlling the architecture of a printed construct, biofabrication approaches hold great promise to capture salient functions of living tissues and guide the maturation of engineered constructs.^[16] In recent years, advancements in the field have led to intraoperative biofabrication, where cell-laden bioinks can be extruded or printed in situ in a surgical setting.^[17,18] For example, PEG hydrogels containing chondrocytes have been directly ink-jet printed into the cartilage defect of an osteochondral plug model *ex vivo*.^[19] Similarly, a handheld extrusion printer has been developed to simultaneously deliver mesenchymal stromal cells (MSCs) and gelatin-methacryloyl (GelMA) hydrogels into chondral defects in a single-session surgery.^[17] Although promising, both studies demonstrated that the integration of the printed constructs to the native host tissue remained a significant issue,^[20] and in general, the in vivo stability and integration of tissue engineered constructs remains a major challenge in the field of cartilage regeneration.^[20–22] Importantly, while stable axial integration can be achieved for treatment strategies targeting osteochondral defect repair, *i.e.*, through anchoring in the subchondral bone,^[20] to achieve a reliable lateral integration within the chondral region is a particularly daunting task. This type of integration is especially challenging when using hydrogels or bioinks that display optimal cell embedding properties and thus low mechanical properties. This is particularly relevant since cells thrive best in hydrogels with low crosslinking density, and stiffer bioinks have been demonstrated to limit neo-cartilage deposition.^[23] Overcoming the limitation imposed by integrating soft hydrogels in situ particularly relevant in the treatment of joint diseases, as poor interconnection between engineered repair tissue and the surrounding native cartilage is a key cause of failure upon cyclic compressive and shear loading exhibited in healthy synovial joints.^[24] Finally, there is also evidence that chondrocyte activity and matrix production and remodeling at a biomaterial–host tissue interface have an effect on lateral integra-

tion of the hydrogel.^[24] Therefore, cell viability in and around the hydrogel is deemed vital for long-term success.

Another important aspect concerning implant integration when injecting or printing hydrogels in situ is the selection of an appropriate crosslinking mechanism for the material. This can impact the viability of the cells encapsulated within it and the interaction with the surrounding native tissue. Ideally, the crosslinking process should be simple, fast, and safe in a clinical setting. Photo-crosslinkable hydrogels can generally be formed rapidly (within seconds to minutes) and on demand, upon exposure to various light sources in the presence of the appropriate photoinitiators. Moreover, light-based reactions offer facile and accurate spatiotemporal control over the physicochemical properties of hydrogels.^[25] As a consequence, these are often common steps in many bioprinting workflows to stabilize printed bioinks and improve the shape fidelity of biofabricated constructs.^[9] Thus, engineer such photochemistry can open new possibilities to introduce new functionalities into bioinks.

A commonly used crosslinking mechanism for most photo-crosslinkable hydrogels is based on free-radical chain-growth and step-growth polymerization,^[26,27] often initiated upon exposure to UV or visible light depending on the selected initiators, such as hydroxy-1-[4-(2-hydroxyethoxy)phenyl]-2-methyl-1-propanone (Irgacure 2959) and lithium phenyl-2,4,6-trimethylbenzoylphosphinate (LAP). There are however major considerations of using UV light in situ, such as the potential damage to cells in the surrounding native tissue, which may impair the restoration of healthy cellular functionality.

The aim of this study was to develop a hydrogel-based cartilage bioink compatible with in situ delivery that could act as a cell carrier, as well as an adhesive gel that is able to bind to cartilage. Importantly, the activation of these multiple functionalities could be achieved in a single step via a biocompatible one-step photo-crosslinking reaction, a process that is compatible with a safe application on native living tissues. GelMA was used as a platform for further modification due to its ability to provide a permissive environment for cell growth and its well-demonstrated applicability for 3D bioprinting applications.^[15,28] Herein, GelMA was further derivatized with tyramine moieties (GelMA-Tyr) that can establish covalent bonds with tyrosine residues present in the extracellular matrix of native tissues. Moreover, a visible light photoinitiating system, based on tris(2,2'-bipyridyl)ruthenium(II) chloride and sodium persulfate (Ru/SPS),^[29] was employed to assess its potential to initiate both the methacryloyl chain-growth polymerization and dityramine bond formation in a single step. This multifunctional, biofunctionalized hydrogel was characterized as a 3D culture environment for cartilage repair, a bioink for bioprinting and as biogluce for binding to the native cartilage.

2. Results and Discussion

2.1. Synthesis of GelMA-Tyr

To produce a hydrogel system carrying two photoresponsive functionalities, GelMA-Tyr was successfully synthesized in two steps as shown by the ¹H-NMR spectra in **Figure 1**, and a schematic of the functionalization step is reported in **Figure 1A**.

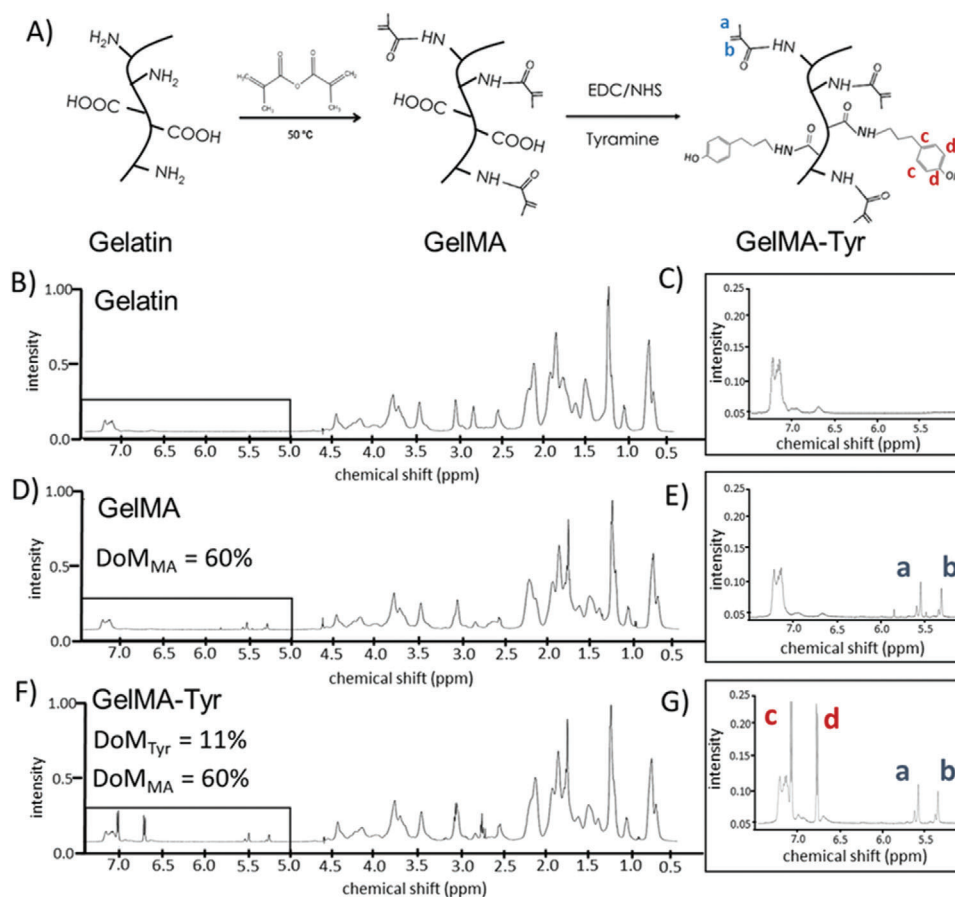


Figure 1. Functionalization process to obtain the dual responsive hydrogels. A) Schematic representation of the synthesis of GelMA and GelMA-Tyr; representative ¹H-NMR spectra of gelatin, GelMA and GelMA-Tyr. B–G) ¹H-NMR spectra of the functionalized hydrogels, showing the presence of the characteristic peaks for acrylates (a,b) in the GelMA and GelMA-Tyr groups and for the added phenolic groups in the GelMA-Tyr polymers.

For GelMA, the degree of modification (DoM) is defined as the percentage of modified lysine groups that are able to react with methacrylic anhydride.^[30] Although methacrylic anhydride can also react with carboxyl and hydroxyl groups, it was previously reported that the primary amine groups have highest reaction affinity with the anhydrides.^[30] When comparing the ¹H-NMR spectra of GelMA to that of gelatin (Figure 1B–E), the presence of proton peaks corresponding to the MA groups can be clearly observed at $\delta = 2.5\text{--}2.6$ ppm. The DoM of methacryloylation (DoM_{MA}) is quantified to be 60%, and is in agreement with previously published studies following similar synthesis protocols.^[24,31,32] The synthesized GelMA was subsequently grafted with tyramine groups onto the GelMA backbone. In this study, a simple carboxyl-amine coupling reaction was employed where Tyr groups were conjugated via their primary amine to the carboxyl moieties of GelMA. ¹H-NMR characterization showed that the reaction was successful as indicated by the presence of extra proton peaks assigned to the Tyr groups at $\delta = 6.8\text{--}7.2$ ppm.^[33,34] In the context of the tyramination reaction, the DoM_{Tyr} was defined as the percentage of modified amino acids containing carboxyl groups (glutamic acid and aspartic acid), and was calculated to be 11% (Figure 1F).^[35] Previous reports have demonstrated the derivation of Tyr groups onto pristine gelatin,

applying a different carboxyl-amine coupling route, in which the Bolton–Hunter reagent (*N*-succinimidyl-3-4-hydroxypropionate) was used as the Tyr carrier.^[36] This reaction however, targets the accessible primary amines (lysine) of gelatin, and is less suitable in our targeted dual functionalization approach, given that the initial methacryloylation reaction also reacts with the lysine moieties. Furthermore, the carboxyl-targeting tyramination reaction was demonstrated to not affect the methacryloyl groups that were already conjugated onto the gelatin backbone, where the DoM_{MA} remained as 60% for GelMA-Tyr. This is particularly important, as the MA groups are known to be highly functional and might react with the reactants and byproducts generated from the tyramination reaction. The DoM_{Tyr} (11%) was deliberately aimed to be lower than DoM_{MA} (60%) by taking into consideration that gelatin already possesses 0.5 mol% native tyrosine groups.^[37] Collectively, these results confirm that it is possible to functionalize gelatin in a dual-step reaction, firstly with MA groups and then by subsequent Tyr moieties, where both the chemical modification processes targeted different grafting sites on gelatin, and hence were compatible with each other. Importantly, this allowed for controlled experiments to be accurately performed to study the application of the dual functionalization in the context of biofabrication.

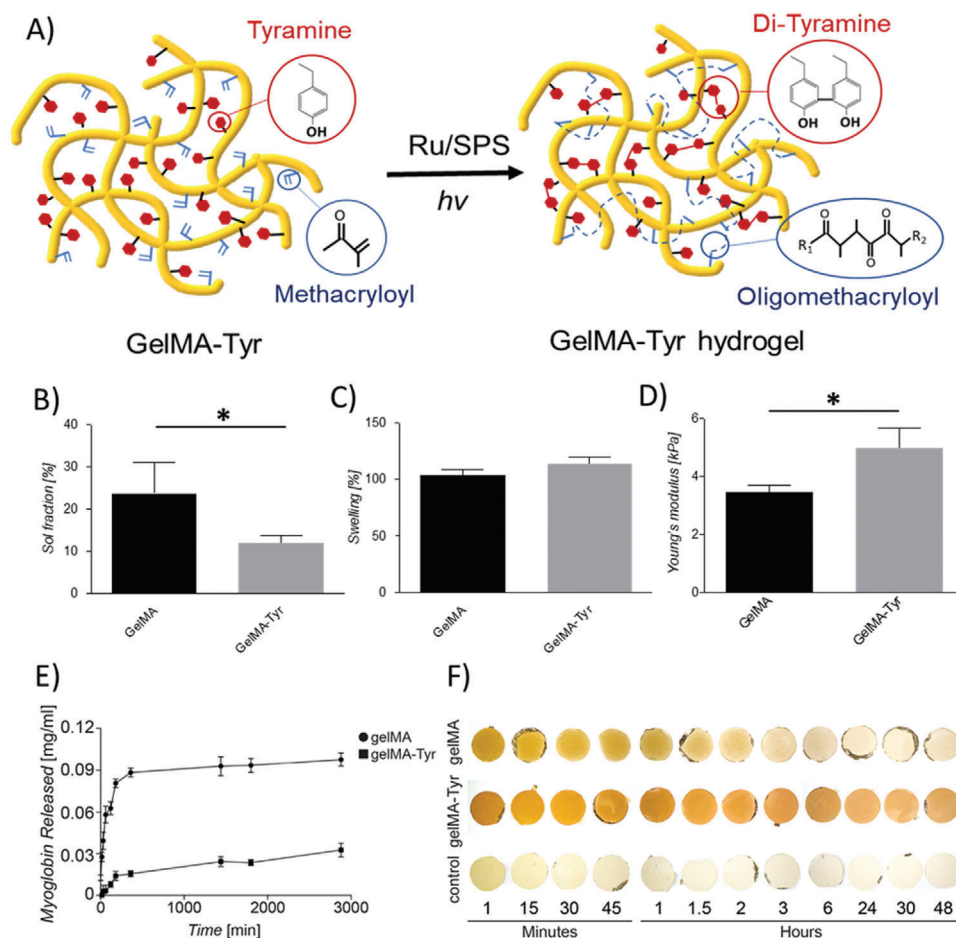


Figure 2. Fabrication and physicochemical and mechanical characterization of the one-step inducible, dual crosslinked hydrogels. A) Schematic representation of the crosslinking process of the GelMA-Tyr macromer. B) Sol fraction values and C) swelling behavior of the hydrogels as observed via sol-gel analysis; D) compressive young's modulus of the casted hydrogels. Incorporation of myoglobin into GelMA or GelMA-Tyr hydrogels: E) release profile of myoglobin from GelMA or GelMA-Tyr hydrogels over 3000 min; F) macroscopic images of GelMA and GelMA-Tyr hydrogels incorporated with myoglobin over 48 h.

2.2. Physicochemical and Mechanical Characterization of GelMA-Tyr Hydrogels

The synthesized GelMA-Tyr macromer was successfully fabricated into hydrogels using the visible light mediated Ru/SPS system (Figure 2A), and was further compared to GelMA hydrogel controls, a well-studied system in biofabrication and common choice in the field of cartilage tissue regeneration.^[12,22,38] Optimization of the photoinitiator content to minimize the sol fraction of the fabricated GelMA-Tyr hydrogels led to selection of 0.5×10^{-3} M Ru and 5×10^{-3} M SPS as the optimal photoinitiator concentration. Mass loss and swelling studies demonstrated that GelMA-Tyr hydrogels had significantly lower sol fraction value (11.9%, $p < 0.05$) than GelMA gels (23.6%, Figure 2B). Ru is a transition metal complex and has been characterized to be highly absorptive in the visible light range ($\epsilon \approx 14\,600 \text{ M}^{-1} \text{ cm}^{-1}$ at 450 nm). When irradiated with visible light, Ru^{2+} becomes photoexcited and then oxidizes into Ru^{3+} , primarily by donating electrons to SPS. After accepting electrons, SPS dissociates into sul-

fate anions and sulfate radicals. For GelMA, these generated sulfate radicals trigger the chain-growth polymerization of the MA groups, forming nondegradable oligomethacryloyl kinetic chains that crosslink the network together.^[24,39] Similarly, these sulfate radicals have been previously shown to also facilitate step-growth thiol-ene polymerization of gelatin-based hydrogels.^[31] However, for GelMA-Tyr, it was hypothesized that in addition to the MA chain-growth polymerization, the photo-oxidized Ru^{3+} could also abstract electrons from the grafted Tyr groups, forming tyrosyl radicals that eventually establish covalent di-tyramine bonds with nearby Tyr moieties.^[36,40,41] This photomediated di-tyramine crosslinking is well characterized and has been previously to fabricate protein hydrogels such as those based on resilin, fibrinogen, and silk.^[42-44] Therefore, it is expected that the GelMA-Tyr hydrogels have a higher crosslinking density as the hydrogel network consists of crosslinks in the form of both oligomethacryloyl kinetic chains and di-tyramine bonds (Figure 2A). Interestingly, both the GelMA and GelMA-Tyr gels showed similar swelling behavior (Figure 2C), where the additional di-tyramine crosslinks

did not affect the overall water uptake capacity of the GelMA-Tyr hydrogels (Figure S1, Supporting Information). The GelMA-Tyr hydrogels also exhibited a significantly higher mechanical compressive modulus (4.98 kPa) compared to GelMA (3.46 kPa, Figure 2D), which is in agreement with previous studies where hydrogels of higher crosslinking density possess higher mechanical stiffness.^[45,46] Moreover, both GelMA and GelMA-Tyr macromers maintained the ability, typical of their common precursor gelatin, to form thermosensitive gels upon cooling at 4 °C, which is then stabilized via photo-crosslinking (Figure S2, Supporting Information). Interestingly, the addition of the tyramine moieties appeared not to modify the susceptibility of the GelMA hydrogel to enzymatic degradation, in presence of collagenase, suggesting that cell mediated remodeling of the gel over time is possible (Figure S3, Supporting Information).

In addition, Ru-mediated di-tyramine and di-tyrosine crosslinking can be used to induce gelation in pristine proteins (Figure S4, Supporting Information). As such, Tyr groups on the dual functionalized GelMA-Tyr system can bind to any phenolic moieties on proteins (i.e., endogenous tyrosine and tryptophan residues), with potential implications to establish controlled release systems. Hence, the ability of GelMA-Tyr to further covalently immobilize proteins within the hydrogel network was evaluated using myoglobin as a model compound, which is rich in tyrosine groups and exhibits a distinct UV-vis absorbance spectrum, facilitating its detection without the need for further modification. It was shown that in GelMA hydrogels, the incorporated myoglobin displayed a burst release profile where approximately all the myoglobin had leached out of the network within the first 4 h of incubation in phosphate buffered saline (PBS). In contrast, the GelMA-Tyr hydrogels showed a significantly higher retention of myoglobin, where 70% of the initially incorporated protein remained within the hydrogel network after 48 h of incubation (Figure 2E). This result was further confirmed with the macroscopic images, where the dark brown color of myoglobin was retained within the GelMA-Tyr hydrogels throughout the 48 h period (Figure 2F). In comparison, the GelMA gels showed a shift in color from dark brown to clear over the incubation period, as a consequence of the rapid release profile of myoglobin (Figure 2F). Importantly, previous research has demonstrated the incorporation of proteins (lysozyme and α -amylase) into hydrogels via similar di-tyrosine/tyramine crosslinking, and showed that upon release, the functionality of these proteins was preserved. These observations suggest that the linked proteins did not undergo denaturation,^[47a] a situation that would facilitate the translation of this light-based system for controlled delivery of bioactive agents. Furthermore, this process is versatile, and can be applied to crosslink or form hydrogels from a wide array of pristine, tyrosine-carrying proteins. To our knowledge, the Ru/SPS system has been applied separately to either crosslink methacryloylated or tyraminated hydrogels biomaterials.^[31,32,36,47a,b] Importantly, in this study, this visible light mediated Ru/SPS system was utilized for the first time to crosslink a dual functionalized polymer/macromer, where both the MA chain-growth polymerization and di-tyramine crosslinking occurred concurrently in a single hydrogel system in one photoexposure step. This phenomenon is a unique advantage of using this Ru/SPS system over other conventional photoinitiating systems such as I2959 or LAP.

2.3. Assessment of In Vitro Chondrogenesis

Given that GelMA-Tyr hydrogels were designed for cell delivery to chondral defects, articular chondroprogenitor cells (ACPCs) were encapsulated into the one-step, dual crosslinked gels, where GelMA hydrogels served as a control. Both the GelMA and GelMA-Tyr hydrogels supported high cell viability (>70%) at 1 and 7 days postfabrication (Figure 3A). This result is in accordance to previously published studies where the Ru/SPS concentration ($0.5 \times 10^{-3}/5 \times 10^{-3}$ M) used in this study is not toxic to cells,^[31,32] as well as to previous work with other light- and enzymatic-activated tyraminated polymers, suggesting no adverse cytotoxicity risk due to undesired interaction with the cell membrane proteins.^[49,50] In order to evaluate the functionality of the encapsulated ACPCs, the cell-laden hydrogels were further cultured in chondrogenic differentiation medium for 28 days. It was observed that the cells embedded within the GelMA-Tyr hydrogels offered a permissive environment for the chondrogenic differentiation of ACPCs, as indicated by a significantly higher GAG/DNA value ($120 \mu\text{g} \mu\text{g}^{-1}$) after 28 days in culture compared to GelMA ($52 \mu\text{g} \mu\text{g}^{-1}$) (Figure 3B). Surprisingly, the compressive modulus of the cell-laden GelMA hydrogels was significantly higher (28 kPa) than the GelMA-Tyr samples (10 kPa), even though both materials showed similar mechanical properties at the beginning of the culture period (Figure S5, Supporting Information). While the mechanical properties of both gels are relatively low for applications in large tissue defects subjected to continuous mechanical loads, several reinforcing strategies based on the combination or coprinting with stiff thermoplastic support scaffolds have already been reported in the literature to address this common limitation for bioinks.^[51-54] Further analysis into the gene expression over the 28 day culture period showed that both collagen type II and type I expression was upregulated in the GelMA and GelMA-Tyr hydrogels (Figure 3D,E). It was also observed that the collagen type II expression is significantly higher in the GelMA-Tyr samples (0.8-fold) after 28 days as compared to GelMA (0.3-fold). There was no significant difference in terms of the collagen type I expression for both 1 and 28 days in the two sample groups. Collagen type II is a well-known marker of native hyaline cartilage while collagen type I is expressed prevalently in fibrocartilage.^[55] Therefore, an higher value for the ratio between the expression levels of collagen type II and type I is generally indicative of a chondrogenic phenotype,^[55-57] and this indicator was found significantly higher in GelMA-Tyr samples (Figure 3E), albeit still lower than 1. A further analysis on the expression of the superficial zone marker PRG4, a key factor in joint lubrication,^[12,58] revealed a higher expression (4-fold) in the GelMA-Tyr samples compared to GelMA (2-fold) after 1 day, but showed a downregulation after 28 days in culture (Figure 3F). Immunohistological analysis confirmed the results of the in vitro biochemical assays, where deposition of glycosaminoglycans (GAGs) (Figure 3G,I), collagen type II (Figure 3H,K) and collagen type I (Figure 3I,L) was observed. Interestingly, albeit collagen I gene expression was relatively high in all samples, at a protein level as detected by immunohistochemistry, this molecule appeared to be less densely present in the neo-cartilage matrix compared to collagen type II, with a higher distribution of collagen type II over collagen type I in both GelMA (5.93 ± 0.95 -fold) and GelMA-Tyr (2.27 ± 1.38 -fold)

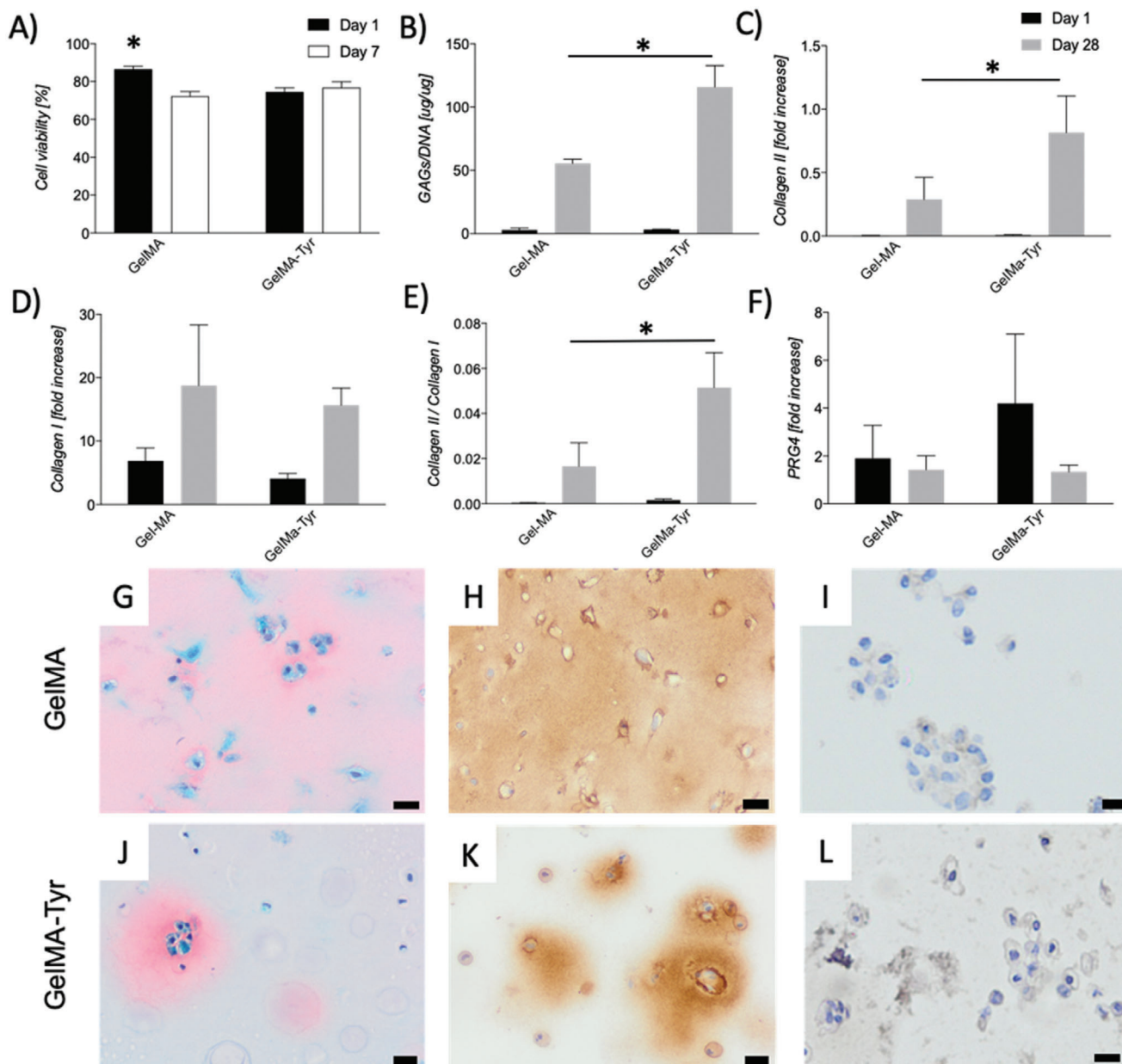


Figure 3. Chondrogenic differentiation of ACPCs encapsulated within GelMA or GelMA-Tyr hydrogels. A) Cell viability after 1 and 7 days in culture. B) GAG/DNA and C) Young's modulus of ACPC-laden GelMA or GelMA-Tyr gels after 1 and 28 days in culture. D) Collagen type II, E) Collagen type I, and F) PRG4 gene expression of ACPC-laden GelMA or GelMA-Tyr gels after 1 and 28 days in culture. Histological stainings of ACPC-laden GelMA or GelMA-Tyr gels after 28 days, G,) safranin-O, H,K) collagen type II, scale bar = 20 μm , and I,L) collagen type I, scale bar = 40 μm .

(Figure S6, Supporting Information), suggesting the differentiation of ACPCs toward a hyaline cartilage-forming phenotype. Overall, quantification from histological sections provides measurements on the distribution of a given ECM component, in terms of area covered. However, it should be noted that unlike the performed biochemical assays, such measurements do not provide a quantitative measurement of the amounts of produced GAGs or collagens. In the analyzed slides GAG and collagen type II distribution was found to be higher in the GelMA group compared to the GelMA-Tyr group (5.09-fold for the GAGs and 2.07-fold for collagen type II). No significant difference was

found for collagen type I in terms of area coverage (Figure S6, Supporting Information). Such results seem to suggest that the extra di-tyramine crosslinking provided by the tyramine moieties at the specific polymer concentration and degree of functionalization tested in this study, on top of that provided by the oligomethacryloyl kinetic chain, may limit the diffusion of neo-secreted ECM moieties. Overall, such inhomogeneous distribution of the neo-synthesized ECM components in the GelMA-Tyr group, which appeared to accumulate prevalently in the pericellular space, may be responsible for the limited stiffening of these hydrogels over the culture time. GelMA

hydrogels have been extensively studied as matrices for cartilage regeneration, where cartilage-relevant cells such as articular chondrocytes, nasal chondrocytes, and chondroprogenitor cells have been encapsulated within GelMA gels and showed good chondrogenic differentiation.^[59–62a] In this study, the focus is instead placed on the extra Tyr groups grafted onto GelMA, and the influence of formation of di-tyramine bonds during the crosslinking reaction on cellular chondrogenic behavior. Initially, it was hypothesized that both GelMA and GelMA-Tyr hydrogels should support similar levels of cartilage regeneration given that the initial swelling behavior ($\approx 100\%$) and mechanical properties (4–6 kPa) were similar. Surprisingly, considerable differences between both the sample groups were observed, where although GelMA-Tyr facilitated chondrogenic differentiation of the embedded ACPCs, based on the indication of quantitative markers such as shown by higher GAG/DNA value and collagen type II expression after 28 days, the immunohistological data showed inhomogenous distribution of the neo-cartilage matrix when compared to GelMA. It can be hypothesized that the GelMA-Tyr hydrogels have higher crosslinking density due to the formation of both oligomethacryloyl kinetic chains and di-tyramine crosslinks, which could hinder the diffusion of neo-matrix. In addition, high crosslinking densities have been previously suggested to impact cellular functions such as mitosis and differentiation,^[62b–d] and previous studies have shown that introduction of secondary covalent crosslinking into hydrogels inhibited the spreading and differentiation of encapsulated mesenchymal stromal cells.^[62c] In this study, the DoM_{MA} was kept constant at 60% for both GelMA and GelMA-Tyr. We anticipate that by reducing the DoM_{MA} for GelMA-Tyr, hydrogels of similar crosslinking density to GelMA can be fabricated, which could be applied to avoid potential drawbacks given by the degree of crosslinking density. Future studies will also focus on covalently incorporating chondrogenic supporting biomolecules into these gels to further enhance the differentiation of the encapsulated cells.^[61] Finally, as the tyramination reaction targets carboxyl containing amino acids such as aspartic and glutamic acid, which are respectively a key component of the cell-attachment RGD sequence (arginine-glycine-aspartic acid) and of the collagen-specific GFOGER sequence, it is speculated that the GelMA-Tyr hydrogels possibly possess less cell-adhesive motifs. This reduction in cell-adhesive sites might indeed contribute to the chondrogenic capacity as indicated in previous studies where less spreading area and lower RGD domain density promote higher extent of chondrogenic differentiation.^[63] Accordingly, other studies also indicated that conjugating RGD sequences onto alginate or hyaluronan hydrogels inhibited *in vitro* chondrogenesis.^[64,65]

2.4. Bioprinting of GelMA-Tyr Hydrogels

The suitability of GelMA-Tyr as a bioink for extrusion 3D bioprinting was further evaluated. While GelMA has been extensively characterized as a bioink for extrusion bioprinting,^[39,66] in this study, we evaluated what effect grafting of Tyr groups onto GelMA had on the printability of the resulting bioink. It was observed that although both materials have shear-thinning properties, GelMA-Tyr displayed a higher complex viscosity compared

to GelMA at low shear rates (10^{-1} to 10^1 Hz, **Figure 4A**). This might be due to the conjugated Tyr groups enhancing the overall hydrophobicity of the macromer solution, which results in a higher solution viscosity. It is well documented that hydrophobic effect is an important phenomenon that drives the interaction between proteins which stabilizes the protein conformation.^[67] Hence, it is logical that GelMA-Tyr, which is more hydrophobic than GelMA, has an increased interaction between the macromer chains and thus requires a higher yield stress to facilitate extrusion of the material. Importantly, ACPCs were able to withstand the shear stress during extrusion where cell-laden GelMA or GelMA-Tyr bionks showed high cell viability ($>70\%$, **Figure 4B**) and sustained metabolic activity (**Figure S7**, Supporting Information) 1 and 7 days postprinting, demonstrating the suitability of the dual functionalized bioinks for applications in such a bioprinting approach. The diameters of printed hydrogel filaments made of GelMA and GelMA-Tyr were comparable and ranged between about $677 \pm 87 \mu\text{m}$ (highest value observed in GelMA prints) to $280 \pm 29 \mu\text{m}$ (lowest value as observed in GelMA-Tyr prints), when increasing the velocity of the collector plate from 3 to 21 mm s^{-1} (**Figure S8**, Supporting Information). Moreover, both GelMA and GelMA-Tyr were able to be extruded into 3D structures which shape was rapidly stabilized by exposure to 450 nm light (**Figure 4C,D**). Even so, occasional and undesired occlusion of the printed pores could be observed (**Figure 4D**), possibly due to relaxation of the extruded hydrogel prior to stabilization by photo-crosslinking. Printing resolution could be further improved, for instance through the use of nozzles with finer gauge, as shown via printing grids of GelMA and GelMA-Tyr using a 27G nozzle (**Figure S9**, Supporting Information), although such choice should be weighed carefully, as recent reports indicated potential detrimental effects in terms of chondrogenic potential of stressed cells sheared through needles with smaller diameters.^[68] Finally, the filament collapse test further showed that both GelMA and GelMA-Tyr filaments could easily span over supporting pillars placed at different distances, even bridging 16 mm gaps, with no noticeable difference between both bioinks.

2.5. Interaction and Integration with Native Cartilage

An exciting translational opportunity for photo-crosslinkable hydrogels is their application intraoperatively, either via minimally invasive injections or through advanced *in situ* bioprinting approaches.^[13,69–71] For this purpose, a carrier system in which the cartilage bioink consisting of GelMA-Tyr and cells can be extruded directly into the chondral defect, followed by photoirradiation to crosslink the hydrogel network is envisioned, while, at the same time, exploiting the applied photochemistry to improve lateral integration into the cartilage region (**Figure 5A**). Such an approach could allow both the delivery of cells to the defect and provide an enhanced integration with the surrounding native cartilage. In terms of photo-crosslinking, most studies have shown that cells can be encapsulated into hydrogels using either UV or visible light irradiation and remain viable and functional after encapsulation.^[38,72] For example, UV-A and near UV wavelengths are known to generate reactive oxygen species and free radicals that can indirectly damage DNA.^[73,74] In this context, hydrogels with gelation chemistries based on radical

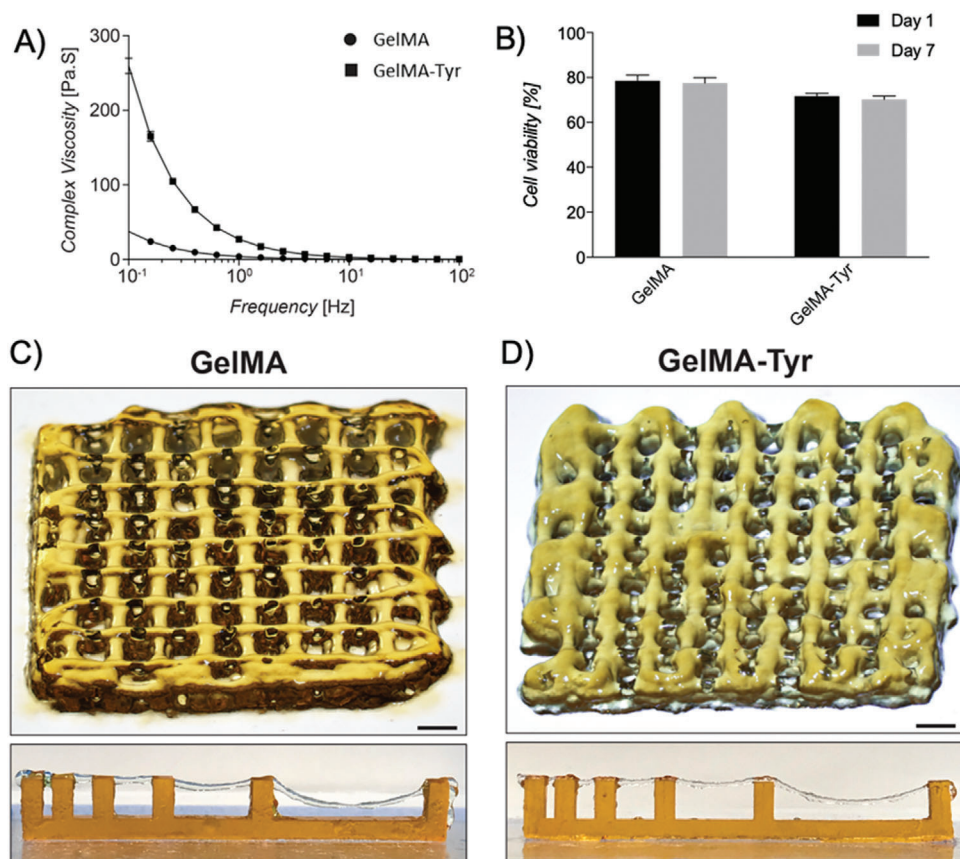


Figure 4. Extrusion bioprinting of GelMA-Tyr bioinks. A) Rheological profile of GelMA and GelMA-Tyr in response to shear rate. B) Cell viability of ACPCs bioprinted within GelMA and GelMA-Tyr constructs. Macroscopic images of extrusion bioprinted C) GelMA and D) GelMA-Tyr constructs, together with a representative image of the filament collapse assay, showing the ability of the printed struts to bridge gaps of 4 mm without noticeable deformation, and up to 16 mm while experiencing sagging. Scale bar = 1 mm.

initiation have been shown to consume such potentially harmful radicals, thus protecting the embedded cells, and allowing to identify safer crosslinking windows.^[38,75] However, in a clinical setting, it can be challenging to confine such photo-crosslinking reactions exclusively to the defect volume. Thus, neighboring healthy tissues, which are not enclosed in such protective hydrogels, may be harmed by harsh light sources. These effects can be more evident for gels based on methacryloyl chemistry (or more broadly on chain growth polymerization) when using photoinitiators which require considerably high irradiation dosages to overcome oxygen inhibition, given by the inherent difficulty of limiting oxygen concentration in an *in vivo*, intraoperative setting. First, the effect of using UV light or visible light on the surrounding cartilage tissue was thus evaluated. LIVE/DEAD images showed that irradiation of cartilage tissue with UV had a dose-dependent detrimental effect on cell viability, whereas high intensity of visible light irradiation had no effect on cell survival within the native cartilage (Figure 5B–F). It was further observed that a high UV irradiation dosage (36 000 mJ cm⁻²), used as negative control, resulted in 100% chondrocyte death in the proximity of the exposed defect, whereas 40% cell-death was observed in samples irradiated with standard UV dosage (1800 mJ cm⁻²) typically used to crosslink GelMA (with I2959) hydrogels in a normoxic environment.^[76,77] On the other hand, the percentage

of normalized live cells in samples irradiated with visible light (14 400 mJ cm⁻²) was not statistically different to that of cartilage biopsies that were not photoexposed (Figure 5B). This was also the case for samples crosslinked with the type I initiator LAP 0.1% w/v, able to initiate the acryloyl-based chain polymerization, upon exposure to a 405 nm light source (Figure S10, Supporting Information). In the field of cartilage engineering and bioprinting, GelMA-based bioinks have been extensively studied to encapsulate cartilage relevant cells (chondrocytes, chondroprogenitors, and MSCs), and have been extensively fabricated using the UV and I2959 system. Although several reports have suggested that such UV-based system is not detrimental to embedded cells during the encapsulation process,^[39] the results presented here showed that UV irradiation can be harmful on the healthy, native tissue surrounding the gel-filled cartilage defects *in vivo*. Hence, the visible light-mediated crosslinking system may be more clinically relevant especially if the cell-laden hydrogels are to be administered intraoperatively.

A key challenge for the *in situ* application of cell-laden hydrogels is that of their retention at the target site and the integration within the native tissue. Herein, the adhesion strength of the cell-laden cartilage bioink to the native tissue was evaluated using a custom-made push-out apparatus (Figure 5G), to assess whether the one-step crosslinking of the dual functionalized

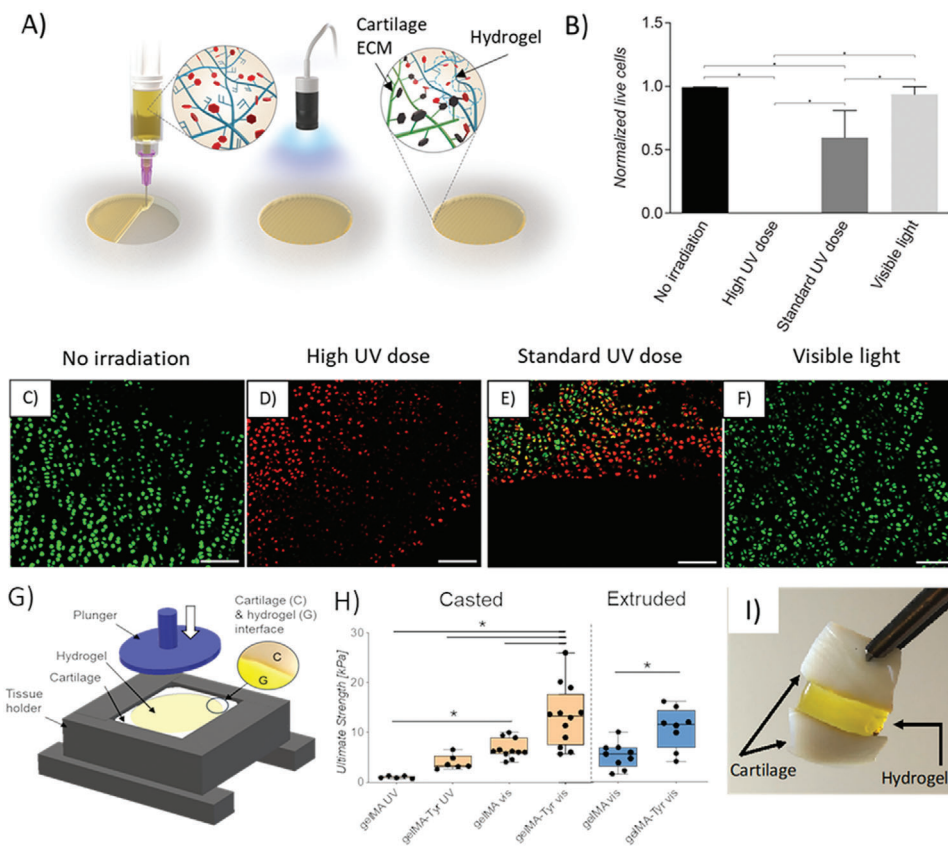


Figure 5. A) Schematic of intraoperative administration of GelMA-Tyr to the chondral defect. B) Normalized amount of live cells and C–F) LIVE/DEAD images of cartilage biopsies irradiated with UV or visible light. Scale bar = 100 μ m. G) Setup of the pushout assay to determine bond-strength. H) Bond-strength of GelMA or GelMA-Tyr administered to the cartilage biopsies as a solution or physically crosslinked gel. I) Cartilage biopsies adhered together using GelMA-Tyr.

GelMA-Tyr could endow the bioinks with tissue-adhesive properties. A simple way to deliver hydrogels into a defect site could be that of casting a prepolymer solution. However, the rapid development of bioprinting technologies has opened new opportunities to print hydrogel-based 3D structures, and pattern multiple cell types for instance, with the goal of recreating the zonal organization of native cartilage.^[12,22] In the context of zonal cartilage regeneration, gelatin bioinks can be initially dispensed in their solution form when using inkjet printing. On the other hand, with the most widely used extrusion-based bioprinting approaches, most gelatin-based bioinks are delivered at low temperature, where the gelatin is first allowed to physically crosslink through hydrogen bonding, then dispensed taking advantage of its shear-thinning properties.^[78] To model both situations, the bond strength between the resulting hydrogel and the surrounding tissue was evaluated for GelMA and GelMA-Tyr macromers administered to chondral defects created on cartilage explants, either via casting or via extrusion through a nozzle, followed by in situ photoirradiation. When cast, the GelMA-Tyr samples exhibited significantly higher bond strength (13.25 kPa) compared to GelMA (6.7 kPa) upon exposure to visible light, indicating enhanced integration with the surrounding native cartilage (Figure 5H). Bond strength was significantly reduced (\approx 15-fold vs GelMA-Tyr with visible light) in hydrogels crosslinked

using a UV 365 nm light source and I2959 photoinitiator. The type-I I2959 photoinitiator was specifically used as a control and it cannot efficiently induce the formation of di-tyramine bonds. Furthermore, when the macromers were extruded as filaments into the defect through a nozzle, the integration of GelMA-Tyr to the native cartilage tissue remained significantly higher compared to GelMA, exhibiting bond strengths of 10.41 ± 4.04 kPa and 5.10 ± 2.51 kPa, respectively ($p = 0.0049$) (Figure 5H). The adhesive capacity of GelMA-Tyr crosslinked with visible light was also visually highlighted by applying a patch of gel as a glue to link two cartilage biopsies together (Figure 5I). Together, these results indicate that the introduction of Tyr groups to GelMA enhanced binding to the surrounding native cartilage through the di-tyramine crosslinking as hypothesized. Gitten et al. previously reported on using chitosan-based hydrogels crosslinked using genipin or rose bengal to improve the binding between the hydrogel and the cartilage interface.^[79] However, such an approach required enzymatic degradation of the cartilage tissue to expose collagen fibers in order to increase the available crosslinking sites at the hydrogel-cartilage interface. Similarly, Broguiere et al. developed factor XIII/transglutaminase crosslinked hyaluronan hydrogels (HA-TG), which showed good stability and adhesiveness to the native cartilage, but also required enzymatic digestion to expose crosslinking sites from the cartilage matrix to achieve

a bond strength of 6 kPa, a value 3-times higher than what found for fibrin glue, a standard fixator in cartilage treatments such as autologous chondrocyte implantation,^[80] yet 2.5 times lower than what found for Ru/SPS crosslinked GelMA-Tyr. In this study, we showed that the visible light-mediated crosslinking of GelMA-Tyr can be administered to chondral defects safely, without the use of detrimental UV light sources or requiring any modification of the host tissue, i.e., via enzymatic digestion strategies, whereby the resultant GelMA-Tyr hydrogels were still able to bind strongly to the surrounding native cartilage.

3. Conclusion

Visible light crosslinkable GelMA-Tyr hydrogels, in combination with Ru/SPS photoinitiators, have potential for the in situ repair of cartilage defects. In particular, thanks to the dual crosslinking mechanism triggered by Ru/SPS, this hydrogel demonstrates potential for direct injection and integration into damaged cartilage. It is also suitable for bioprinting applications, further enhancing its possibilities for the repair or replacement of complex, patient-specific structures. This versatile system also enables grafting of unmodified proteins onto the bioink backbone through a one-step photoexposure process, potentially enabling the applicability of this ink for controlled protein release and for further applications in biofunctionalization. Overall, the combination of Ru/SPS-mediated visible light crosslinking and dual functionalized (bio)inks could be expanded to a wide range of biocompatible materials and has potential for intraoperative bioprinting applications.

4. Experimental Section

Synthesis of GelMA and GelMA-Tyr: All materials were obtained from Sigma-Aldrich and used without further modification, unless stated otherwise. GelMA was synthesized by adding 0.6 g of methacrylic anhydride per gram of gelatin (type A, from porcine skin, 10 w/v% in PBS), and left to react for 1 h at 50 °C under constant stirring, as previously described.^[81] The resultant GelMA solution was then dialyzed against deionized water at 40 °C to remove unreacted methacrylic anhydride and byproducts. For the synthesis of GelMA-Tyr and tyramine-modified gelatin (Gel-Tyr, used as control for the dual functionalization process), tyramine groups were coupled to the carboxyl groups of GelMA (or pristine gelatin) using carbodiimide chemistry. GelMA (10% w/v in 2-(N-morpholino)ethanesulfonic acid), MES buffer) was reacted with 1-ethyl-3-(3-dimethylaminopropyl)carbodiimide (EDC, 1.5×10^{-3} mol L⁻¹) and N-hydroxysuccinimide (NHS, 0.75×10^{-3} mol L⁻¹) for 15 min at 40 °C, followed by addition of tyramine (36.5×10^{-3} mol L⁻¹), then left to react for another 24 h at 40 °C with gentle stirring. The resultant GelMA-Tyr solution was then dialyzed against deionized water at 40 °C. All purified macromer solutions were sterile filtered (0.22 µm), freeze-dried, and stored at 4 °C.

Nuclear Magnetic Resonance: The DoM was quantified using ¹H-proton nuclear magnetic resonance (NMR; Bruker Avance 400 MHz). GelMA, Gel-Tyr, or GelMA-Tyr were dissolved in deuterium oxide (D₂O) and analyzed using ¹H NMR (300 MHz Bruker Avance DPX-300 spectrometer). For GelMA, DoM_{MA} is defined as the percentage of modified amino acid groups containing primary amines that reacted with methacrylic anhydride. The area of methacryloyl (MA) proton peaks, $\delta = 2.5\text{--}2.6$ ppm, was compared to the area of the phenylalanine protons in the gelatin backbone. For Gel-Tyr and GelMA-Tyr, DoM with tyramine (DoM_{Tyr}) is defined as the percentage of modified amino acids that contain carboxylic groups. The area of the tyramine (Tyr) proton peaks,

$\delta = 6.8\text{--}7.2$ ppm, was compared to the peaks corresponding to the phenylalanine groups. The composition of acid-treated porcine skin gelatin was acquired from the gelatin handbook of the gelatin manufacturer institute of America (GMIA).^[82] The phenylalanine peaks at $\delta = 7.2\text{--}7.4$ ppm were used as reference signals for both the methacryloylation and tyramination, and were calibrated to 10.5 protons as this amino acid's content in the used gelatin is 2.1%.

Preparation and Characterization of Casted Hydrogel: Lyophilized GelMA and GelMA-Tyr were dissolved at 8% w/v in PBS at 37 °C. Photoinitiators (Ru and SPS) were added to the different macromer solutions at a $0.5 \times 10^{-3}/5 \times 10^{-3}$ M final concentration. Hydrogel discs (6 mm in diameter \times 2 mm in height) were created by crosslinking in open air using a visible light lamp for 8 min at 30 mW cm⁻². Sol and gel fractions as well as swelling studies were performed as previously described ($n = 6$).^[83] An unconfined uniaxial compression test was performed by applying $\sim 20\%$ min⁻¹ strain rate with a dynamic mechanical analyzer (DMA Q800, TA Instruments, The Netherlands). The compression modulus was calculated as the slope of the stress/strain curve in the 10–15% strain range. The degradability of both GelMA and GelMA-Tyr hydrogels was assessed via incubation in a 0.15% w/v solution of collagenase type II in Dulbecco's modified Eagle medium (DMEM, 31966, Gibco, The Netherlands), supplemented with 10% v/v heat-inactivated fetal bovine serum (FBS Gibco, The Netherlands), and 1% v/v penicillin and streptomycin (Life Technologies, The Netherlands). Samples ($n = 3$ per time point) were freeze dried at different time points of incubation (10, 20, 30, 45, and 60 min), and the mass loss was measured compared to that of pristine, as-casted hydrogels.

In Vitro Biological Evaluation: All animal-derived materials were obtained from deceased horses donated to science with informed consent from their owner, and in accordance with the Ethical Guidelines of the University Medical Center Utrecht and the Faculty of Veterinary Medicine of Utrecht University. Equine ACPCs were isolated as previously reported,^[15] expanded in culture to passage 3 in ACPC expansion medium consisting of DMEM supplemented with 10% v/v FBS, 1% v/v penicillin and streptomycin (Life Technologies, The Netherlands), 1% MEM nonessential amino acids solution (NEAA, Gibco, The Netherlands), and 5 ng mL⁻¹ basic fibroblast growth factor (bFGF, Peprotech, UK). ACPCs were then resuspended in 8% w/v GelMA and GelMA-Tyr hydrogels at a concentration of 20×10^6 cells mL⁻¹, and then irradiated with visible light. Hydrogel samples were cultured in chondrogenic differentiation medium (DMEM, supplemented with 1% insulin–transferrin–selenous acid (ITS+ Premix, Corning, USA), 0.2×10^{-3} M ascorbic acid-2-phosphate, 1% v/v penicillin and streptomycin, 100×10^{-9} M dexamethasone, and 10 ng mL⁻¹ transforming growth factor- β 1 (TGF- β 1). Medium was refreshed 3 times a week. Cell viability was assessed at day 1 and day 7 using a LIVE/DEAD assay (calcein AM, ethidium homodimer-1, Life Technologies, The Netherlands) ($n = 3$) and taking images with a confocal laser scanning microscope (Leica SP8X, Leica Microsystems, Germany). Cell laden GelMA and GelMA-Tyr hydrogels were harvested at day 1 and 28 for further analysis. Neocartilage formation was evaluated by sulfated GAGs and DNA quantification ($n = 3$). GAGs were quantified through a dimethylmethylene blue assay (DMMB, Sigma Aldrich, The Netherlands). DNA content was measured using a Quanti-iT PicoGreen dsDNA kit (Life Technologies, The Netherlands). Gene expression was analyzed by quantitative polymerase chain reaction (qPCR) ($n = 3$). ACPC-laden hydrogels were harvested and mechanically ground in RLT buffer (Qiagen, Germany). The lysate was processed with the RNeasy Mini kit (Qiagen, Germany) in order to isolate mRNA. A Superscript III Platinum SYBR Green One-Step qRT-PCR Kit (Life Technologies, The Netherlands) was used for amplification and cDNA synthesis. The relative expression levels for collagen type I (COL1A1), collagen type II (COL2A1), and proteoglycan 4 (PRG4) were analyzed compared to the housekeeping gene hypoxanthine phosphoribosyltransferase-1 (HPRT1), using primers that have been previously described.^[15] Relative expression, Ct, and efficiency values were calculated using the PCR Miner algorithm.^[84] For histological analysis, the hydrogel samples were fixed in formalin and embedded in paraffin ($n = 3$). 5 µm sections were stained to visualize cartilage matrix production via Safranin-O staining for sGAG content and immunohistochemistry for both collagen type I (sc-8784, Santa Cruz

Biotechnology, USA) and collagen type II (DSHB, II-II6B3, USA). For the quantitative assessment of the area covered by each ECM component, for each staining, three different slides were selected randomly from the samples ($n = 3$). Microscopy images were converted to binary images via thresholding with the software ImageJ, and the percentage of the area covered by the staining in pixels was calculated.

Myoglobin-Binding Assay: To test the potential of GelMA-Tyr as a carrier of biomolecules, 10% w/v GelMA and 10% w/v GelMA-Tyr solutions were supplemented with 10 mg mL⁻¹ equine muscle-derived myoglobin and cast into cylindrical samples as previously described ($n = 3$). For these experiments, the oxidized form of myoglobin (metmyoglobin) was utilized. Myoglobin-free samples were included as controls. After crosslinking, samples were incubated at 37 °C in DPBS to assess protein release over a 48 h time span (after 1, 15, 30, and 45 min and 1, 1.5, 2, 3, 6, 24, 30, and 48 h). At each time point, the hydrogel samples were collected for stereomicroscopy imaging and the media was analyzed with a UV-vis spectrometer (Lambda 35, Perkin Elmer, USA) to quantify the amount of globin myoglobin over a wavelength range of $\lambda = 360\text{--}460$ nm. Myoglobin concentrations were derived from the peak absorbance value at 409 nm of using a standard curve.^[85]

Rheometry: The rheological properties of the hydrogel precursor solutions were assessed using a DHR2 rheometer (TA Instruments, The Netherlands). A stainless-steel flat plate (diameter = 40 mm) with a 60 μ m plate-to-plate distance was used for all rheological tests. GelMA and GelMA-Tyr solutions were loaded and their complex viscosity was recorded at 21 °C as a function of shear rate (0.01–100 Hz), after two cooling (5 min at 4 °C) and recovery (5 min at 21 °C) conditioning cycles, at a constant strain of 5% ($n = 5$).

Hydrogel Printability: The GelMA or GelMA-Tyr macromers were loaded in a pneumatic-driven, extrusion-based printing system (23G stainless-steel nozzle, extrusion pressure between 1.9 and 2.5 bar, printing temperature = 18 °C, 3DDiscovery, regenHU, Switzerland). The effect of increasing the collector velocity (feed rate) from 3 to 21 mm s⁻¹ on the diameter of the printed filaments was assessed, printing several straight lines ($n = 3$) and measuring their diameter from microscopy images using ImageJ software. In order to assess the printability of the solutions, a filament collapse test was also performed as previously described using photoinitiator-free gel and images were captured using a digital camera to visualize the extent of the spanning filaments ($n = 5$).^[86] These prints were made using a feed rate ranging from 15 to 25 mm s⁻¹. A 5-layered, 10 \times 10 mm square grid with 1 mm interfilament spacing was also printed with each hydrogel blend to assess the stacking ability of the gels ($n = 5$). In order to stabilize the extruded filaments, the hydrogel solutions were supplemented with $0.5 \times 10^{-3}/5 \times 10^{-3}$ M Ru/SPS and were irradiated during the printing process, and for 5 min postprinting to ensure polymerization of the printed constructs. The printed grids were imaged with a stereomicroscope (Olympus SZ2-ILST, Olympus Corporation, Japan).

Evaluating Hydrogel Blends as Potential Bioinks for Bioprinting: ACPCs were harvested at passage 3 and embedded in GelMA and GelMA-Tyr inks at a density of 20×10^6 cells mL⁻¹. These cell-laden hydrogel solutions were supplemented with $0.5 \times 10^{-3}/5 \times 10^{-3}$ M Ru/SPS. Bioprinting was performed with the previously described extrusion-based system, with the same nozzle and temperature, and under the same visible light crosslinking conditions described in Section 2.7. Printed cylindrical samples (diameter = 5 mm, height = 1 mm) were cultured in ACPC expansion medium for 7 days. Cast controls were fabricated as previously described using the same cell density and crosslinking conditions. Medium was refreshed twice per week. Samples were analyzed for cell viability through a LIVE/DEAD assay and measuring their metabolic activity through a resazurin assay (resazurin salt, Alfa Aesar, Germany) after 1 and 7 days of culture ($n = 3$).

In Situ Photo-Crosslinking and Effects on the Native Cartilage: To evaluate the impact photoexposure on the tissue surrounding the implanted hydrogel constructs, equine cartilage samples of about 1 cm² were freshly harvested from fetlock joints postmortem. Using a biopsy punch, 4 mm defects were made in the center of the explants, filled with 8% GelMA-Tyr and photoexposed. Hydrogel-free, nonirradiated explants with a punched chondral defect were used as positive controls. Ru/SPS gels crosslinked

with visible light were compared to Irgacure crosslinked with either high ($36\,000$ mJ cm⁻², negative control) or a standard (1800 mJ cm⁻²) UV dose (365 nm, Vilber-Lourmat 144 portable UV-lamp, France) ($n = 3$). The standard dose represented the minimum necessary to crosslink the hydrogels in nontoxic conditions. Cartilage explants were subjected to a LIVE/DEAD assay.

Adhesion of the Bioink to Cartilage: To evaluate the adhesion strength of GelMA and GelMA-Tyr hydrogels to native cartilage tissue, a push-out test was carried out. Cartilage discs of 10 mm in diameter and 1.5–2 mm in thickness were obtained from equine stifle joints. The cartilage disks were fixed in between two custom-made holders, and a cylindrical defect (4 mm) was imparted in the center of the explant using a biopsy punch. GelMA and GelMA-Tyr hydrogel solutions, together with Ru/SPS ($0.5 \times 10^{-3}/5 \times 10^{-3}$ M) were cast into the defects at a concentration of 8% gel and exposed to visible light for 10 min ($n = 11\text{--}12$). After incubation in PBS, a mechanical push-out test performed with a custom-made clamp in a Dynamic Mechanical Analyzer (DMA, TA Instruments, USA) was used to measure the adhesion strength between the hydrogels and the native cartilage. A force ramp of 0.1 N min⁻¹ (no preload) was applied until failure. The thickness of each cartilage disk was measured with a digital caliper in order to calculate the interface area. The ultimate push-out stress was calculated by dividing the static force by the interface area ($2\pi rh$). As controls, GelMA and GelMA-Tyr hydrogels were also prepared using 0.1% w/v Irgacure 2959 and UV-crosslinked with 1800 mJ cm⁻² ($n = 5\text{--}6$). Furthermore, to assess the binding of the bioink in an in situ printing setting, GelMA and GelMA-Tyr bioinks were loaded in a syringe and let undergo thermal gelation at 4 °C ($n = 8\text{--}9$). Subsequently, after being equalized at the printing temperature, the bioinks were extruded (23G nozzle) as filaments to fill the chondral defect, and crosslinked with visible light in presence of Ru/SPS, incubated in PBS and finally subjected to the push-out tests.

Statistical Analysis: Results were reported as mean \pm standard deviation. Statistical analyses were performed using GraphPad Prism 7.0 (GraphPad Software, USA). For the quantitative data, single comparisons were assessed via a Student's *t*-test, and multiple comparisons with a one-way ANOVA, followed by post hoc Bonferroni correction to test differences between groups. When normality could not be assumed, nonparametric tests were performed (Mann–Whitney for single comparisons and Kruskal–Wallis for multiple comparisons). Differences were found to be significant when $p < 0.05$.

Supporting Information

Supporting Information is available from the Wiley Online Library or from the author.

Acknowledgements

K.S.L. and F.A. contributed equally to this work. The authors would like to thank Anneloes Mensinga and Mattie van Rijen for their support with the qPCR and histological analysis. F.A., P.N.B., J.M., and R.L. acknowledge the funding from the Dutch Arthritis Society (LLP-12 and LLP-22), the European Research Council (grant agreement #647426, 3DJOINT), from the EU-Horizon 2020 research and innovation program under the grant agreement #814444 (MEFISTO), and from the AO Foundation (OCD consortium, Reinforce project). K.S.L. acknowledges funding by New Zealand Health Research Council (Emerging Researcher First Grant – 15/483, Sir Charles Hercus Health Research Fellowship – 19/135) and Royal Society of New Zealand (Marsden Fast Start – MFP-UOO1826). T.B.F.W. acknowledges funding from Royal Society of New Zealand (Rutherford Discovery Fellowship – RDF-UOO1204).

Conflict of Interest

The authors declare no conflict of interest.

Keywords

biofabrication, biogluce, bioprinting, cartilage tissue engineering, tissue integration

Received: December 13, 2019

Revised: March 8, 2020

Published online: April 23, 2020

- [1] D. C. Flanigan, J. D. Harris, T. Q. Trinh, R. A. Siston, R. H. Brophy, *Med. Sci. Sports Exercise* **2010**, *42*, 1795.
- [2] a) A. E. Wluka, C. Ding, G. Jones, F. M. Cicuttini, *Rheumatology* **44**, 1311, **2005**; b) V. H. M. Mouser, N. M. M Dautzenberg, R. Levato, M. H. P. van Rijen, W. Dhert, J. Malda, D. Gawlitta, *ALTEX* **2018**, *35*, 65.
- [3] E. B. Hunziker, *Osteoarthritis Cartilage* **2002**, *10*, 432.
- [4] S. L. Vega, M. Y. Kwon, J. A. Burdick, *Eur. Cells Mater.* **2017**, *33*, 59.
- [5] J. Li, G. Chen, X. Xu, P. Abdou, Q. Jiang, D. Shi, Z. Gu, *Regener. Biomater.* **2019**, *6*, 129.
- [6] a) Regentis Biomaterials, GelrinC; b) Medipost, CARTISTEM.
- [7] E. Schuh, S. Hofmann, K. S. Stok, H. Notbohm, R. Müller, N. Rotter, *J. Tissue Eng. Regener. Med.* **2012**, *6*, e31.
- [8] B. S. Schon, G. J. Hooper, T. B. F. Woodfield, *Ann. Biomed. Eng.* **2017**, *45*, 100.
- [9] J. Malda, J. Visser, F. P. Melchels, T. Jüngst, W. E. Hennink, W. J. A. Dhert, J. Groll, D. W. Huttmacher, *Adv. Mater.* **2013**, *25*, 5011.
- [10] K. S. Lim, M. Baptista, S. Moon, T. B. F. Woodfield, J. Rnjak-Kovacina, *Trends Biotechnol.* **2019**, *37*, 1189.
- [11] W. M. Groen, P. Diloksumpan, P. R. van Weeren, R. Levato, J. Malda, *J. Orthop. Res.* **2017**, *35*, 2089.
- [12] V. H. M. Mouser, R. Levato, L. J. Bonassar, D. D. D'Lima, D. A. Grande, T. J. Klein, D. B. F. Saris, M. Zenobi-Wong, D. Gawlitta, J. Malda, *Cartilage* **2017**, *8*, 327.
- [13] A. C. Daly, F. E. Freeman, T. Gonzalez-Fernandez, S. E. Critchley, J. Nulty, D. Kelly, *Adv. Healthcare Mater.* **2017**, *6*, 1700298.
- [14] A. Kosiz-Kozioł, M. Costantini, A. Mróz, J. Idaszek, M. Heljak, J. Jaroszewicz, E. Kijeńska, K. Szöke, N. Frerker, A. Barbetta, J. E. Brinckmann, W. Świączkowski, *Biofabrication* **2019**, *11*, 035016.
- [15] R. Levato, W. R. Webb, I. A. Otto, A. Mensinga, Y. Zhang, M. van Rijen, R. van Weeren, I. M. Khan, J. Malda, *Acta Biomater.* **2017**, *61*, 41.
- [16] R. Levato, T. Jüngst, R. Scheurer, T. Blunk, J. Groll, J. Malda, *Adv. Mater.* **2020**, 1906423, <https://doi.org/10.1002/adma.201906423>.
- [17] C. Di Bella, S. Duchi, C. D. O'Connell, R. Blanchard, C. Augustine, Z. Yue, F. Thompson, C. Richards, S. Beirne, C. Onofrillo, S. H. Bauquier, S. D. Ryan, P. Pivonka, G. G. Wallace, P. F. Choong, *J. Tissue Eng. Regener. Med.* **2018**, *12*, 611.
- [18] S. V. Murphy, P. De Coppi, A. Atala, *Nat. Biomed. Eng.* **2019**, <https://doi.org/10.1038/s41551-019-0471-7>.
- [19] X. Cui, K. Breitenkamp, M. G. Finn, M. Lotz, D. D. D'Lima, *Tissue Eng., Part A* **2012**, *18*, 1304.
- [20] I. A. D. Mancini, R. A. Vindas Bolaños, H. Brommer, M. Castilho, A. Ribeiro, J. P. A. M. Van Loon, A. Mensinga, M. H. P. Van Rijen, J. Malda, R. Van Weeren, *Tissue Eng., Part C* **2017**, *23*, 804.
- [21] K. L. Spiller, S. A. Maher, A. M. Lowman, *Tissue Eng., Part B* **17**, 281, **2011**.
- [22] I. M. Khan, S. J. Gilbert, S. K. Singhrao, V. C. Duance, C. W. Archer, *Eur. Cells Mater.* **2008**, *16*, 26.
- [23] V. H. M. Mouser, F. P. Melchels, J. Visser, W. J. Dhert, D. Gawlitta, J. Malda, *Biofabrication* **2016**, *8*, 035003.
- [24] M. A. DiMicco, R. L. Sah, *J. Orthop. Res.* **19**, 1105, **2001**.
- [25] C. Chung, J. Mesa, M. A. Randolph, M. Yaremchuk, J. A. Burdick, *J. Biomed. Mater. Res., Part A* **2006**, *77A*, 518.
- [26] C. E. Hoyle, C. N. Bowman, *Angew. Chem., Int. Ed.* **2010**, *49*, 1540.
- [27] B. D. Fairbanks, M. P. Schwartz, C. N. Bowman, K. S. Anseth, *Biomaterials* **2009**, *30*, 6702.
- [28] J. Idaszek, M. Costantini, T. A. Karlsen, J. Jaroszewicz, C. Colosi, S. Testa, E. Fornetti, S. Bernardini, M. Seta, K. Kasarello, R. Wrzesien, S. Cannata, A. Barbetta, C. Gargioli, J. E. Brinckmann, W. Świączkowski, *Biofabrication* **2019**, *11*, 044101.
- [29] J. W. Bjork, S. L. Johnson, R. T. Tranquillo, *Biomaterials* **2011**, *32*, 2479.
- [30] K. Yue, X. Li, K. Schrobback, A. Sheikhi, N. Annabi, J. Leijten, W. Zhang, Y. S. Zhang, D. W. Huttmacher, T. J. Klein, A. Khademhosseini, *Biomaterials* **2017**, *139*, 163.
- [31] S. Bertlein, G. Brown, K. S. Lim, T. Jüngst, T. Boeck, T. Blunk, J. Tessmar, G. J. Hooper, T. B. F. Woodfield, J. Groll, *Adv. Mater.* **2017**, *29*, 1703404.
- [32] K. S. Lim, B. J. Klotz, G. C. J. Lindberg, F. P. W. Melchels, G. J. Hooper, J. Malda, D. Gawlitta, T. B. F. Woodfield, *Macromol. Biosci.* **2019**, *19*, 1900098.
- [33] K. S. Lim, J. J. Roberts, M. H. Alves, L. A. Poole-Warren, P. J. Martens, *J. Appl. Polym. Sci.* **2015**, *132*, 42142.
- [34] K. S. Lim, M. H. Alves, L. A. Poole-Warren, P. J. Martens, *Biomaterials* **2013**, *34*, 7907.
- [35] J. Van Hoorick, P. Gruber, M. Markovic, M. Tromayer, J. Van Erps, H. Thienpont, R. Liska, A. Ovsianikov, P. Dubrue, S. Van Vlierberghe, *Biomacromolecules* **2017**, *18*, 3260.
- [36] C. M. Elvin, T. Vuocolo, A. G. Brownlee, L. Sando, M. G. Huson, N. E. Liyou, P. R. Stockwell, R. E. Lyons, M. Kim, G. A. Edwards, G. Johnson, G. A. McFarland, J. A. M. Ramshaw, J. A. Werkmeister, *Biomaterials* **31**, 8323, **2010**.
- [37] W. G. Cobbett, A. W. Kenchington, A. G. Ward, *Biochem. J.* **1962**, *84*, 468.
- [38] M. Bartnikowski, N. J. Bartnikowski, M. A. Woodruff, K. Schrobback, T. J. Klein, *Acta Biomater.* **2015**, *27*, 66.
- [39] B. J. Klotz, D. Gawlitta, A. J. W. P. Rosenberg, J. Malda, F. P. W. Melchels, *Trends Biotechnol.* **2016**, *34*, 394.
- [40] D. A. Fancy, C. Denison, K. Kim, Y. Xie, T. Holdeman, F. Amini, T. Kodadek, *Chem. Biol.* **2000**, *7*, 697.
- [41] D. A. Fancy, T. Kodadek, *Proc. Natl. Acad. Sci. USA* **1999**, *96*, 6020.
- [42] C. M. Elvin, A. G. Carr, M. G. Huson, J. M. Maxwell, R. D. Pearson, T. Vuocolo, B. E. Liyou, D. C. Wong, D. J. Merritt, N. E. Dixon, *Nature* **2005**, *437*, 999.
- [43] C. M. Elvin, A. G. Brownlee, M. G. Huson, T. A. Tebb, M. Kim, R. E. Lyons, T. Vuocolo, N. E. Liyou, T. C. Hughes, J. A. M. Ramshaw, J. A. Werkmeister, *Biomaterials* **2009**, *30*, 2059.
- [44] X. Cui, B. G. Soliman, C. R. Alcalá-Orozco, J. Li, M. A. M. Vis, M. Santos, S. G. Wise, R. Levato, J. Malda, T. B. F. Woodfield, J. Rnjak-Kovacina, K. S. Lim, *Adv. Healthcare Mater.* **2020**, *9*, 1901667.
- [45] H.-J. Kong, K. Y. Lee, D. J. Mooney, *Polymer* **2002**, *43*, 6239.
- [46] C. B. Hutson, J. W. Nichol, H. Aubin, H. Bae, S. Yamanlar, S. Al-Haque, S. T. Koshy, A. Khademhosseini, *Tissue Eng., Part A* **2011**, *17*, 1713.
- [47] a) F. Lee, J. E. Chung, M. Kurisawa, *J. Controlled Release* **2009**, *134*, 186; b) L. Sando, S. Danon, A. G. Brownlee, R. J. McCulloch, J. A. M. Ramshaw, C. M. Elvin, J. A. Werkmeister, *J. Tissue Eng. Regener. Med.* **2011**, *5*, 337.
- [48] C. M. Elvin, S. J. Danon, A. G. Brownlee, J. F. White, M. Hickey, N. E. Liyou, G. A. Edwards, J. A. M. Ramshaw, J. A. Werkmeister, *J. Biomed. Mater. Res. A* **2010**, *93*, 687.
- [49] C. Loebel, S. E. Szczesny, B. D. Cosgrove, M. Alini, M. Zenobi-Wong, R. L. Mauck, D. Eglin, *Biomacromolecules* **2017**, *18*, 855.
- [50] E. Jooybar, M. J. Abdekhodaie, M. Alvi, A. Mousavi, M. Karperien, P. J. Dijkstra, *Acta Biomater.* **2019**, *83*, 233.
- [51] G. Bahcecioglu, B. Bilgen, N. Hasirci, V. Hasirci, *Biomaterials* **2019**, *218*, 119361.
- [52] V. H. M. Mouser, F. P. W. Melchels, J. Visser, W. J. A. Dhert, D. Gawlitta, J. Malda, *Biofabrication* **2016**, *8*, 035003.

- [53] W. Schuurman, V. Khristov, M. W. Pot, P. R. Van Weeren, W. J. A. Dhert, J. Malda, *Biofabrication* **2011**, 3, 021001.
- [54] M. de Ruijter, A. Ribeiro, I. Dokter, M. Castilho, J. Malda, *Adv. Healthcare Mater.* **2019**, 8, 1800418.
- [55] S. W. O'Driscoll, C. N. Commisso, J. S. Fitzsimmons, *Osteoarthritis Cartilage* **1995**, 3, 197.
- [56] T. B. F. Woodfield, S. Miot, I. Martin, C. A. van Blitterswijk, J. Riesle, *Biomaterials* **2006**, 27, 1043.
- [57] K. Schrobback, T. J. Klein, T. B. Woodfield, *Tissue Eng., Part A* **2015**, 21, 1785.
- [58] G. D. Jay, K. A. Waller, *Matrix Biol.* **2014**, 39, 17.
- [59] S. Pahoff, C. Meinert, O. Bas, L. Nguyen, T. J. Klein, D. W. Hutmacher, *J. Mater. Chem. B* **2019**, 7, 1761.
- [60] V. H. M. Mouser, A. Abbadessa, R. Levato, W. E. Hennink, T. Vermonden, D. Gawlitta, J. Malda, *Biofabrication* **2017**, 9, 015026.
- [61] G. C. J. Brown, K. S. Lim, B. L. Farrugia, G. J. Hooper, T. B. F. Woodfield, *Macromol. Biosci.* **2017**, 17, 1700158.
- [62] a) V. H. M. Mouser, R. Levato, A. Mensinga, W. J. A. Dhert, D. Gawlitta, J. Malda, *Connect. Tissue Res.* 61, 137, **2020**; b) S. Nam, O. Chaudhuri, *Nat. Phys.* **2018**, 14, 621; c) K. Zhang, Q. Feng, J. Xu, F. Tian, K. W. K. Yeung, L. Bian, *Adv. Funct. Mater.* **2018**, 30, 1701642; d) Q. Feng, K. Wei, Z. Xu, Y. Sun, P. Shi, G. Li, L. Bian, *Biomaterials* **2016**, 101, 217.
- [63] Z. Li, B. Cao, X. Wang, K. Ye, S. Li, J. Ding, *J. Mater. Chem. B* **2015**, 3, 5197.
- [64] S. L. Vega, M. Y. Kwon, K. H. Song, C. Wang, R. L. Mauck, L. Han, J. A. Burdick, *Nat. Commun.* **2018**, 9, 614.
- [65] J. T. Connelly, A. J. García, M. E. Levenston, *Biomaterials* **2007**, 28, 1071.
- [66] G. Ying, N. Jiang, C. Yu, Y. S. Zhang, *Bio-Des. Manuf.* **2018**, 1, 215.
- [67] T. Hong, K. Iwashita, K. Shiraki, *Curr. Protein Pept. Sci.* **2018**, 19, 746.
- [68] M. Muller, E. Ozturk, O. Arlov, P. Gatenholm, M. Zenobi-Wong, *Ann. Biomed. Eng.* **2017**, 45, 210.
- [69] C. D. O'Connell, C. Di Bella, F. Thompson, C. Augustine, S. Beirne, R. Cornock, C. J. Richards, J. Chung, S. Gambhir, Z. Yue, J. Bourke, B. Zhang, A. Taylor, A. Quigley, R. Kapsa, P. Choong, G. G. Wallace, *Biofabrication* 015019, **2016**, 8.
- [70] L. Li, F. Yu, J. Shi, S. Shen, H. Teng, J. Yang, X. Wang, Q. Jiang, *Sci. Rep.* **2017**, 7, 9416.
- [71] S. Shen, M. Chen, W. Guo, H. Li, X. Li, S. Huang, X. Luo, Z. Wang, Y. Wen, Z. Yuan, B. Zhang, L. Peng, C. Gao, Q. Guo, S. Liu, N. Zhuo, *Tissue Eng., Part B* **2019**, 25, 187.
- [72] N. E. Fedorovich, M. H. Oudshoorn, D. van Geemen, W. E. Hennink, J. Alblas, W. J. A. Dhert, *Biomaterials* **2009**, 30, 344.
- [73] F. R. de Gruijl, H. J. van Kranen, L. H. F. Mullenders, *J. Photochem. Photobiol., B* **2001**, 63, 19.
- [74] R. Masuma, S. Kashima, M. Kurasaki, T. Okuno, *J. Photochem. Photobiol., B* **2013**, 125, 202.
- [75] E. R. Ruskowitz, C. A. Deforest, *ACS Biomater. Sci. Eng.* **2019**, 5, 2111.
- [76] A. Abbadessa, V. H. M. Mouser, M. M. Blokzijl, D. Gawlitta, W. J. A. Dhert, W. E. Hennink, J. Malda, T. Vermonden, *Biomacromolecules* **2016**, 17, 2137.
- [77] P. Zhuang, W. L. Ng, J. An, C. K. Chua, L. P. Tan, *PLoS One* **2019**, 14, e0216776.
- [78] T. Billiet, E. Gevaert, T. De Schryver, M. Cornelissen, P. Dubruel, *Biomaterials* **2014**, 35, 49.
- [79] J. Gittens, A. M. Haleem, S. Grenier, N. A. Smyth, C. P. Hannon, K. A. Ross, P. A. Torzilli, J. G. Kennedy, *J. Orthop. Res.* 34, 1139, **2016**.
- [80] N. Broguiere, E. Cavalli, G. M. Salzmann, L. A. Applegate, M. Zenobi-Wong, *ACS Biomater. Sci. Eng.* 2, 2176, **2016**.
- [81] K. S. Lim, B. S. Schon, N. V. Mekhileri, G. C. J. Brown, C. M. Chia, S. Prabakar, G. J. Hooper, T. B. F. Woodfield, *ACS Biomater. Sci. Eng.* **2016**, 2, 1752.
- [82] Gelatin Manufacturers Institute of America, *Gelatin Handbook*, GMIA, New York **2012**.
- [83] K. S. Lim, R. Levato, P. F. Costa, M. D. Castilho, C. R. Alcalá-Orozco, K. M. A. Van Dorenmalen, F. P. W. Melchels, D. Gawlitta, G. J. Hooper, J. Malda, T. B. F. Woodfield, *Biofabrication* **2018**, 10, 034101.
- [84] S. Zhao, R. D. Fernald, *J. Comput. Biol.* **2005**, 12, 1047.
- [85] J. P. K. Armstrong, R. Shakur, J. P. Horne, S. C. Dickinson, C. T. Armstrong, K. Lau, J. Kadiwala, R. Lowe, A. Seddon, S. Mann, J. L. R. Anderson, A. W. Perriman, A. P. Hollander, *Nat. Commun.* 6, **2015**, 7405.
- [86] A. Ribeiro, M. M. Blokzijl, R. Levato, C. W. Visser, M. Castilho, W. E. Hennink, T. Vermonden, J. Malda, *Biofabrication* **2017**, 10, 014102.